Chapter 6

The Particle Encapsulation Process

Jose Ignacio Huertas

Additional information is available at the end of the chapter

http://dx.doi.org/10.5772/62019

The aim of this chapter is to model and study the encapsulation process described in Chapter 1 as an alternative to control contamination and agglomeration of flame-synthesized nanosized particles. The aerosol formed during the production of nanosized powders in sodium/halide flames is composed of M, NaCl, and Ar, where M is a metal or ceramic. This type of aerosol is characterized by very high particle concentrations (~10^{18} particles/m^3) and high temperatures (>1000°C). Furthermore, the M/NaCl/Ar aerosol is a two-component aerosol, since both M and NaCl are condensable phases.

Particle formation in flame is affected by many factors that make a complete analysis of this process extremely complicated. Particle dynamics, chemical kinetics, heat and mass transfer fields are some of the factors that affect the final product. Despite these complications, considerable insight can be gained by focusing attention on aerosol dynamics alone and considering the burner as an idealized plug flow reactor in which the relevant gas-phase chemistry and transport are decoupled from the particle dynamics. The characteristics of the final particles, for example, size distribution and morphology, are primarily affected by coagulation and condensation, i.e., by aerosol dynamics.

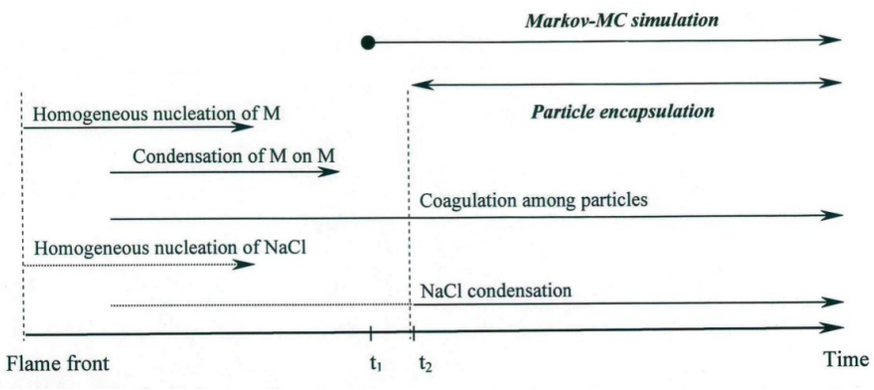

Figure 1. Chronology of events occurring during particle formation in M/NaCl/Ar aerosols. Dashed lines indicate the processes that need to be suppressed to favor encapsulation of M particles.

Particle formation in M/NaCl/Ar aerosols involves the formation and growth of M and NaCl particles by nucleation, condensation, and coagulation. Figure 1 illustrates the processes involved and their sequence. Since NaCl is the more volatile material, encapsulation of M particles will occur, either directly when the NaCl vapor condenses onto the M particles producing NaCl-coated M particles, or indirectly when uncoated particles coagulate with the coated particles.

To describe the evolution of the aerosol when condensing NaCl vapor encapsulates the M particles, the Markov-MC model developed in Chapters 4 and 5 is applied to the M/NaCl/Ar aerosol. This work leads to identifying the controlling mechanisms and variables that affect the particle size distribution (PSD) and the M particles size distribution (MPSD). Furthermore, the model allows the optimum conditions for particle encapsulation to be identified.

1. General description of the aerosol process in a sodium/halide flame

Consider the case where reactant gases MCl_m and Na diluted in inert are mixed and react producing a flame. The products of combustion are the primary (core) material M (e.g., Ti), inert (e.g., Ar), and a condensable material, NaCl, which will serve as the encapsulating material. The overall chemistry for this class of exothermic reactions is:

$$MCl_m + mNa \rightarrow mNaCl + M \tag{1}$$

In the flame sheet limit, the flame can be considered as an infinitesimally thin surface where reactions take place at an infinite rate. The products of combustion form the M/NaCl/Ar combustion aerosol. The temperature of the particles within the aerosol is approximately equal to the temperature of the surrounding gases. The flame temperatures considered can be well below the melting point of the metal or ceramic M. For example, for TiC_4, Na and 90% Ar introduced at 700°C and a pressure of 1 atm, the adiabatic flame temperature is 1053°C. The products of combustion under these conditions are Ti in solid phase (T_m = 1668°C for Ti) and NaCl in vapor phase.

When the temperature of the aerosol is well below the saturation temperature of the M material, it nucleates and condenses. However, under these circumstances, classical homogeneous nucleation theory may not model accurately the nucleation and condensation of the M material, since this theory uses macroscopic physical properties to describe entities made of few atoms. However, since the encapsulation process is not directly affected by nucleation of M, here it is simply assumed that nucleation and condensation of M has been completed well before the onset of NaCl condensation. An. initial size distribution for M will be assumed and the importance of this assumed distribution to the conclusions will be evaluated. Figure 1 illustrates the processes that will be included in the encapsulation study. In the vicinity of the flame front, the NaCl vapor is unsaturated, and therefore coagulation of the M particles is the dominant process. Downstream of the flame front the temperature drops due to heat transfer and heat loss. When the aerosol temperature drops below the NaCl saturation temperature,

http://dx.doi.org/10.5772/62019

the vapor condenses onto the M particles producing NaCl-coated M particles. However, not all the existing particles are coated as explained below.

According to the classical theory of homogeneous condensation, supersaturated vapors will condense if appropriate nuclei are present. The vapor can either create its own nuclei (homogeneous nucleation) or use the existing particles in the aerosol as nuclei of condensation (heterogeneous condensation). The Kelvin effect, discussed in Chapter 5, requires that only nuclei with size greater than a critical size r* can serve as condensation nuclei (r* is defined by Equation 1 from Chapter 5). When S is higher than a critical value (S_{crit}), the concentration of clusters of size r* that are self-generated by the vapor becomes significant and catastrophic homogeneous nucleation occurs (expressions for S_{crit} can be found in Reference 79). On the other hand, when S is less than S_{crit} the number of clusters of size r > r* is negligible. Therefore, for a given temperature, a metastable condition is maintained and condensation will not occur. For the case considered, when the M particles grow to size r > r*, heterogeneous condensation will occur over these "core" particles producing NaCl-coated M particles.

Temperature and vapor concentration of the condensable material must thus be controlled to avoid homogeneous nucleation of NaCl and favor encapsulation of particles through heterogeneous condensation. Rates of heterogeneous condensation must also be fast enough to ensure heavy coatings before subsequent collisions. This type of coating will separate the cores from each other during subsequent collisions, inhibiting the agglomeration of M particles. The range of temperatures and partial pressures of NaCl for which the encapsulation process can occur as described above can be understood by referring to Figure 2. To the right of the saturation pressure curve, NaCl is in a stable unsaturated condition (S<l) and will not condense out regardless of the core particle size. To the left of the homogeneous nucleation curve, NaCl is in a supersaturated condition such that $S>S_{crit}$ and NaCl can form its own nuclei and homogeneously condense out. Between these two curves ($1<S<S_{crit}$) heterogeneous condensation can take place.

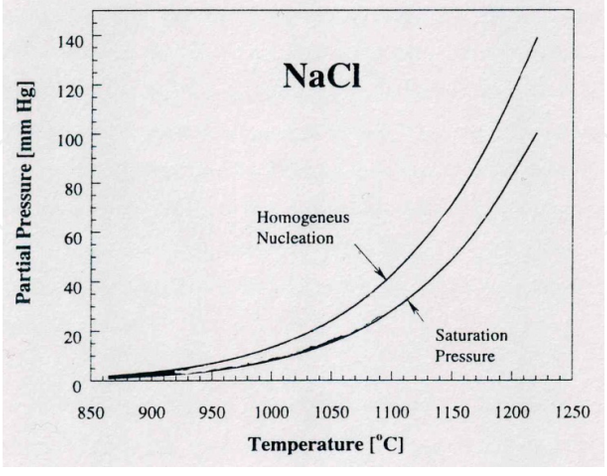

Figure 2. Homogeneous nucleation and saturation pressure curves for NaCl. To the right of the saturation pressure curve, NaCl is unsaturated (S<1) and cannot condense out. To the left of the homogeneous nucleation curve, NaCl is supersaturated ($S>S_{crit}$) and will homogeneously condense out. Between these two curves ($1<S<S_{crit}$) heterogeneous condensation can take place.

While the above discussion is useful in conceptualizing the encapsulation process, particle dynamics has not been considered. In the next section, a more accurate description is obtained by simulating condensation and condensation with the Markov-MC model.

2. Modeling particle encapsulation

The particle encapsulation process in its simplest form is a two-component process that involves two phenomena: particle coagulation and vapor-phase condensation. The governing equations, physical description, and methods of solution for these two processes were presented in Chapters 4 and 5. The modeling of the particle encapsulation process reduces to solving the governing equation through the Markov-MC model under appropriate assumptions and conditions. The description of these assumptions and conditions follows.

2.1. Particle morphology

When two coated particles collide they stick together with a probability α, which is known as the accommodation coefficient. At the contact point of the two spheres, a neck is formed whose size increases with time. For the initial stage, the rate of growth is driven by the curvature gradients in the neck region. For intermediate sintering or coalescing rates, the curvature gradient diminishes and the surface free energy becomes the driving force for continued sintering. At this stage, the motion is induced by the tendency of the interface to reduce its area in order to minimize the interfacial energy. Appendix B presents a description about the mechanisms of particle sintering in microscopic materials. Nonetheless, this information provides an insight in the mechanisms of sintering of nanosized particles.

When the rate of sintering ($1/\tau_{sint}$) of a newly formed particle is much higher than the rate of particle collision, i.e., $\tau_{sint} << \tau_{coll}$, it can be assumed that at any time during the aerosol evolution, the particles are spherical. For uncoated M particles, the spheroidicity of the particles is limited by the rate of sintering of these particles. For coated particles, it is limited by the rate of sintering of the condensed phase, e.g., NaCl. Table 1 shows the characteristic time for sintering of Ti and W in crystal phase and NaCl in liquid phase for several values of particle size. The characteristic times for sintering were obtained assuming that the Ti and W sinter by solid-state diffusion, while NaCl particles coalesce by the viscous flow mechanism. Table 1 shows that the rates of sintering for NaCl droplets and Ti crystal particles are several orders of magnitude faster than collision rates. Then, for the size range considered, it can be concluded that the spheroidicity of the particles is a reasonable assumption. Table 1 also shows that for Ti at 1100°C, particles with size r < 50 nm poses a characteristic sintering time several orders of magnitude shorter than typical experimental resident times (~1s). Thus, no agglomerated structures should be formed while the particle size is 20–40 nm in radii. This conclusion agrees with the SEM and TEM micrographs presented in Chapter 2.

According to the previous discussion, it will be assumed than the particles in the M/NaCl/Ar aerosol are spherical and consist of M cores particles embedded within a NaCl droplet. A

Size r [nm]	τ_{coll} [μs]	τ_{sint} [μs]	
		Ti (c)	NaCl (l)
3.8	214	0.01	$3.73x10^{-3}$
5.9	674	0.04	$5.78x10^{-3}$
15.0	730	0.71	$1.45x10^{-2}$
50.0	1380	27.2	$4.90x10^{-2}$
100.0	5530	216.0	$9.76x10^{-2}$

Table 1. Characteristic time for sintering of Ti particles in crystal phase and NaCl in liquid phase at 1100°C, compared to the characteristic time for collision of Ti particles at 1100°C. $N_{Ti} = 10^{18}$ particles/m^3 when r = 3.8 nm.

particle is described by its equivalent size r and its composition Y, where r is the radius of the particle as a whole and Y is the ratio of NaCl mass and the total mass in the particle. The condition Y = 0 describes a pure M particle, while Y = 1 a pure NaCl particle. When either a coated and uncoated particle or two coated particles collide, two types of structures are possible as shown in Figure 3.

In the first type, NaCl mass fraction of the colliding particles is low ($Y \rightarrow 0$) and the two cores are in contact upon collision. Assuming that the sintering of the two cores is nearly instantaneous, a new spherical particle is formed with size and composition determined by the size and composition of the colliding particles.

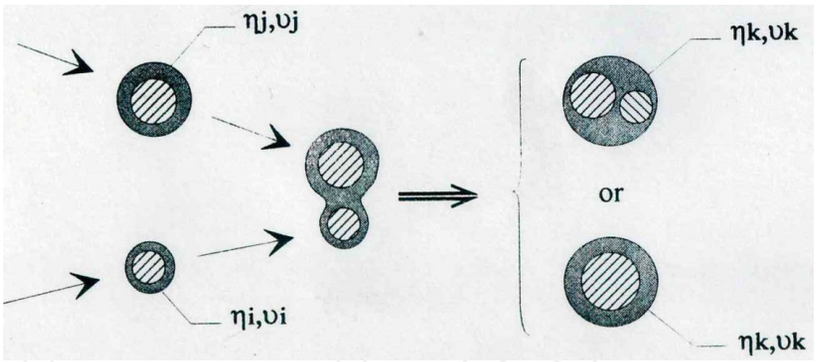

Figure 3. Possible structures formed after collision of particles.

In the second type, the NaCl mass fraction of the colliding particles is high ($Y \rightarrow 1$). The heavy coating on one or both of the particles isolates the cores from each other. The liquid-phase coating of the newly formed particle coalesces instantaneously and a spherical particle with two cores is formed.

However, the cores within the liquid NaCl droplet are subject to Brownian motion and can potentially collide and sinter. Whether the cores within the liquid phase collide or not depends on several factors: NaCl mass fraction (Y), core sizes (r_c), residence time (τ_{res}), and temperature (T) are the dominant ones. T affects the rate of Brownian motion, while Y affects the length scale for collision, yielding a timescale for collision of cores in the liquid phase τ_B. The condition ($Y \rightarrow 1$) combined with ($\tau_{res} \rightarrow 0$) favors final double core particles.

A criterion to determine the amount of coating material required to avoid embedded-core collisions can be obtained from relating the characteristic two-core collision time τ_B to the particle residence time $\tau_{res.}$ The residence time is defined as the time spent by the particle at temperatures higher than that of the melting point of the condensable material. For typical experimental conditions the order of magnitude of τ_{res} is ~ 1s. The condition $\tau_B << \tau_{res}$ leads to the potential that the core particles will contact one another within the NaCl matrix, while $\tau_B >> \tau_{res}$ leads to two separate core particles.

To evaluate the likelihood that the cores will collide, the theory of particle coagulation is applied to a colloidal system made of two equal-sized cores encapsulated in a liquid droplet. The average time for the two cores to collide τ_B is defined in Appendix C as $\tau_B = \mu\pi r^3/8KT$, where r is the total size of the final particle (core plus coating). This model neglects the enhancing effect of the boundaries of the liquid droplet in the rate of collision of the two cores. The model shows that τ_B is independent of the initial core size, and has a linear variation with the volume available for motion of the cores. Table 2 shows the values obtained at different conditions of temperature, and particle size. From Table 2 it can be concluded that the cores within the NaCl liquid droplet collide in a timescale similar to the timescale for collision of the particles in the aerosol, i.e., $\tau_B \sim \tau_{coll.}$ Though the particle diffusion velocities are much lower in the liquid phase, the distances between particles are also much lower.

This approximate analysis also predicts that two Ti cores within NaCl droplets of size r < 100 nm will come in contact within a timescale much shorter than the typical experimental residence time. Whether or not these core particles will sinter or coalesce depends on the conditions within the droplet. Experimental results suggest that low melting point metals (e.g., Ti) coalesce, while hotter melting point materials (e.g., AlN) do not show evidence of sintering and appear to remain as separate core particles. The behavior of core particles upon low velocity collision in a salt matrix will require more attention but is beyond the scope of this work.

(NaCl+M) Droplet of Size r [nm]	τ_B [μs]	
	1100°C	800°C
10	$9.38x10^{-1}$	$1.27x10^{0}$
25	$1.47x10^{1}$	$1.98x10^{1}$
50	$1.17x10^{2}$	$1.58x10^{2}$
100	$9.38x10^{2}$	$1.27x10^{3}$
250	$1.47x10^{4}$	$1.98x10^{4}$

Table 2. Characteristic time for collision of two equal-sized core particles encapsulated within an (NaCl+M) droplet of size r.

Much insight can be gained by considering extreme conditions, i.e., assuming that 1) the cores always collide and coalesce (equilibrium solution) and 2) the cores never collide or coalesce

http://dx.doi.org/10.5772/62019

(frozen solution). The equilibrium solution refers to the results obtained when it is assumed that upon collision of coated particles, a new coated particle with a single core is formed, while the frozen solution refers to the results obtained when it is assumed that the NaCl particle coating prevents collisions or sintering of the cores of the colliding particles. The equilibrium solution overestimates the size of the cores because it enhances coagulation of M cores while the frozen solution underestimates the size because it limits coagulation of the M cores.

2.2. Particle heating during condensation

The theory of condensation described in Chapter 5 assumes constant temperature aerosols. However, particles warm up as the latent heat of vaporization is released during the process of condensation. Usually it is argued that the increase in temperature is negligible, but most of these arguments are for modest condensation rates and for particles in the CR. This issue becomes even more important when it is realized that the rate of condensation is a strong function of S, and S at the particle surface is a strong function of particle temperature. For example, a 3.2°C change in temperature of NaCl vapor at 1100°C decreases S from 1.01 to 0.98. Thus, small temperature variations could result in a very different condensation behavior. Figure 4 illustrates the variation in S when a constant mass of vapor changes temperature.

To characterize the magnitude of the particle temperature increase during condensation, a heat transfer model was developed for both regimes, FMR and CR (see Appendix A). Here, only the conclusions for the FMR are described. As a first step, the analysis assumes that the conditions of the vapor far from the particle remain constant. An energy balance is performed and the resulting equation is solved coupled to the rate of condensation equation.

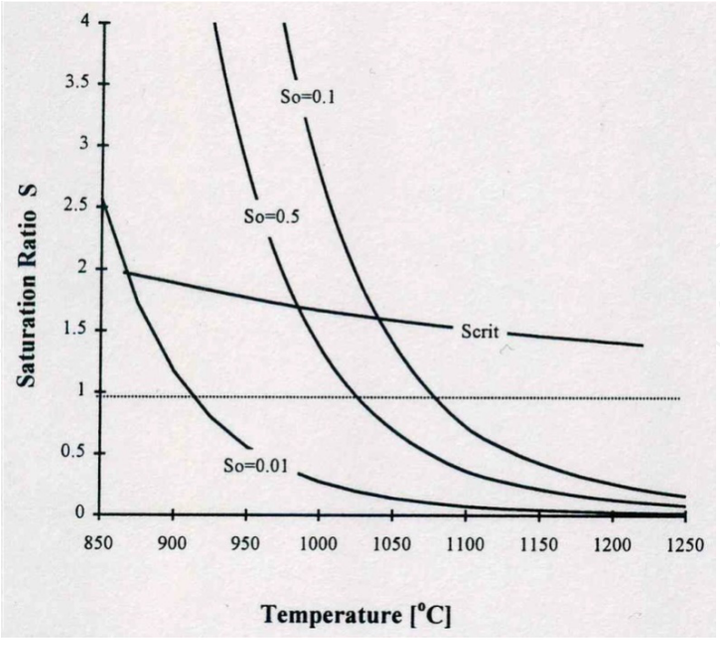

Figure 4. Variation of the saturation ratio (S) with temperature for the same mass of NaCl. S_o is the saturation ratio at 1250°C.

Figure 5 shows the increase in temperature of a Ti particle with size r* as it grows by condensation of NaCl vapor at 1100°C when the rate of condensation is affected by particle heating. The condensation process rapidly approaches a steady-state condition, where the rate of convective heat loss balances the rate of latent heat released. The steady-state condition is established because the thermal resistance of the coated particle is much less than the convective thermal resistance and because the fraction of the energy released needed to heat the coated particle is negligible. Thus, the particle heats instantaneously and the system does not have thermal inertia.

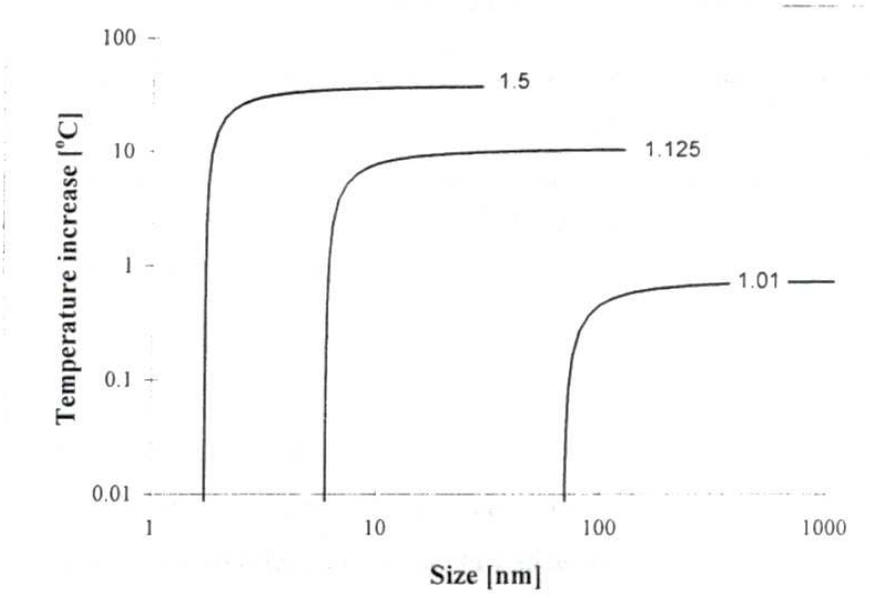

Figure 5. Increase in temperature for Ti particle during condensation of NaCl vapor at 1100°C and S = 1.5, 1.125, and 1.010.

Figure 5 can be understood as follows: energy dissipation by convection is proportional to the increase in particle temperature δT, where $\delta T = T_p - T_\infty$, and the rate of heat release is proportional to the rate of condensation. Thus, δT is proportional to the rate of condensation. The rate of condensation is affected by the Kelvin effect when r~r*, and is thus a function of particle size.

Consequently, for a given S and T, the increase in particle temperature δT is a function of size and there is a unique δT for given size.

The rate of condensation in the FMR is independent of particle size when the Kelvin effect is negligible, and thus a steady-state condition is reached when the particles are sufficiently large. At this state, the particles assume a constant maximum temperature δT_{max} independent of particle size and despite further condensation. The results of Figure 5 and Table 3 show that particles in the FMR undergo a significant increase in temperature for high values of S_∞, i.e., for high rates of condensation. They also shows that neglecting particle heating the growth by condensation is overestimated by a factor of ~4.

S_∞	δT_{max}	m	$m_{w/o}/m$
1.01	0.81	0.25	3.88
1.125	9.86	0.23	4.00
1.5	37.5	0.18	4.44

m = rate of condensation in the FMR when the Kelvin effect is negligible

w/o = without correction for particle heating

Table 3. Particle temperature increase in FMR with particle heating for NaCl at 1100°C.

Thus far, only the local effects of the latent heat release during high rates of condensation have been considered. This energy heats the particles and, consequently, limits the rate of condensation. Another limiting effect on the rate of condensation is found when the global effect of the latent heat release is considered. In adiabatic systems or in systems where the rate of heat loss (q_{loss}) is smaller than the rate of latent heat release, the entire aerosol heats up during the condensation process, as described by the following energy balance:

$$H_v \sum_i n_i \rho_i \frac{dv_i}{dt} = q_{loss} + \sum_i m_i C_{pi} \frac{dT}{dt} \tag{2}$$

where H_v is the latent heat release per unit mass, ρ_i is the density of i in condensed phase, dv_i / dt is the rate of condensation for size I, m_i is total mass of i per unit volume of aerosol where i represents each species in the aerosol including inert, vapor, and condensed phases, and T the global temperature of the aerosol.

As shown in Figure 4, when the global temperature increases, the saturation ratio (S) decreases. The rate of condensation would decrease with time in an adiabatic system, and thus, heat loss plays a critical role in defining the rate of condensation. These two effects were incorporated in the Markov-MC model.

2.3. Wetting effects

When heterogeneous condensation occurs, the condensable phase condenses out on particles made of a different material. The vapor and molecular clusters of the condensable material are absorbed onto the surface of the "foreign" particles, wetting the surface. Once the foreign particles possess a thin coating, the vapor phase does not recognize the identity of the foreign particles and the particles behave as nuclei made of the condensable material. Then condensation proceeds as predicted by the growth law equations described in Chapter 5.

The assumption of this description is that a wetted foreign particle can be obtained. However, hydrophobic solid surfaces are not wetted in such a way that a continuous stable liquid film is formed. The extent of wetting is given by the difference between adhesive (solid–liquid interface) and cohesive (liquid–liquid) forces, and thus a very diverse wetting phenomenon

can be observed depending on the materials involved. The study of particle wetting is out of the scope of this work. Herein it is assumed that the onset of heterogeneous condensation is unaffected by wetting effects, i.e., the condensation growth laws are applicable to the uncoated particles. This assumption implies that NaCl wets the primary particles and that the cohesive forces are negligible compared to the adhesive forces. Figure 2-9 shows a NaCl-encapsulated Ti particle indicating that NaCl effectively wets Ti particles.

2.4. Working regime

For typical experimental conditions of M/NaCl/Ar aerosols, $0.01 < Kn < 10.0$. Therefore, the well-known Fuchs-Sutugin correction factor for condensation and coagulation in the transition regime was included. Implementation of more accurate correlations is straightforward.

2.5. Initial conditions

The controlling variables of the particle encapsulation process in sodium/halide flames are inlet temperature and reactant concentrations. Flame temperature, M mass, and NaCl concentration are determined by stoichiometry, energy conservation, mass conservation, and physical properties of the constituents. Therefore, T and S at the flame front can be taken as the controlling variables for simplicity in the study of the aerosol dynamics.

When NaCl is the encapsulating material, the range of temperatures of interest for atmospheric pressure flames is between 800°C and 1400°C. Flame temperatures can be controlled by reactant dilution and/or by controlling the temperature and phase of the reactants at the inlet of the reactor. Values for the saturation ratio of the condensable vapor range from 1 to S_{crit}. For NaCl, S = 2 is the upper boundary for S_{crit} over a wide range of temperatures as shown in Figure 4.

On the other hand, when the initial S and T are defined, the total mass of the M material is given by stoichiometry. The concentration of M particles (N) is obtained by assuming a particle size distribution (e.g., monodisperse, normal or lognormal) and mass conservation. The initial distribution for the M particles is simply assumed since it is not necessary to accurately predict nucleation to model encapsulation. For each of the cases studied, several runs were made to observe the effect of the initial particle size distribution on the evolution of the aerosol. For the same mass, normal and lognormal distributions were used as the initial condition. For most of the cases the results were qualitatively similar. Therefore, for every case studied, only a typical behavior is presented and discussed.

3. Results

This section presents the results obtained when the Markov-MC model is applied to a Ti/NaCl/Ar aerosol under the assumptions and range of initial conditions described above. This study is intended to allow for an understanding of the dominant mechanism involved in the nanoencapsulation process and to demonstrate the usefulness of the model in studying two-

component aerosols. Two cases will be considered: constant temperature and constant heat loss. The constant temperature case will be considered to introduce the salient features of nanoencapsulation; nonetheless, heat loss which is intrinsic to most flame systems, will be shown to be of fundamental importance in controlling nano-encapsulation.

The results are not expected to yield quantitative agreement with the experiments as the flame has a complex two-dimensional structure and we will assume a uniform aerosol that evolves with time. Nonetheless, we expect the model to elucidate the essential features of nano-encapsulation. We will study the nano-encapsulation process for one case that is similar to the typical conditions of the sodium/halide flame for which there are experimental results as shown in Chapter 2.

3.1. Encapsulation at constant temperature

The constant temperature condition applies to very dilute aerosols or to systems where the rate of latent heat release can be dissipated as it is generated. As an initial study, we will consider the case where a sudden encapsulation occurs in the preexisting aerosol. The aerosol will be subjected to a step change in saturation ratio as might be experienced in flames, expansion shock waves, mixing, or sudden drops in temperature. The main characteristics of the encapsulation process under these conditions will be delineated by considering the evolution of a Ti/NaCl/Ar combustion aerosol. Initially, the aerosol is assumed to consist of a lognormal distribution of pure Ti particles in a supersaturated gas-phase mixture of NaCl with S = 1.125 and T = 1100°C. The parameters of the lognormal distribution are r_m = l.86 nm, σ_g = 1.45. For these conditions, the total particle concentration is N = 1.6 x 10 ^{19} particles/m^3.

Figure 6 shows the evolution of the aerosol. Under the chosen initial conditions $r^* > r_m$ and only the upper tail of the distribution is initially affected by condensation. Since the Kelvin effect mandates that condensation growth rates are lower for smaller particles, condensation elongates the upper tail of the distribution and creates a gap around r*. At the same time, the concentration of the vapor decreases, r* increases, and the rate of condensation slows down. Coagulation fills in the gap and increases the concentration of particles in the upper tail, creating a bimodal distribution. Since the global temperature of the aerosol remains constant and there is no source of condensing material, condensation soon ceases to be important, and coagulation becomes the dominant process. Eventually, coagulation smoothes the distribution, and it approaches a lognormal type.

Figure 7 shows the variation with time of S and r*. It is seen from the figure that condensation is only important for a short initial period of time. S changes from 1.125 to ~1.02 within one millisecond. After that, a condition of slight supersaturation remains during the entire evolution. Condensation occurs at low rates and only over the larger particles. As condensation proceeds, r* increases and fewer particles receive condensation. When these few particles become substantially larger, the collision of these particles with the smaller particles in the distribution becomes favored, and thus the larger particles become sinks for smaller particles. Thus, the larger particles grow due to preferential coagulation and preferential condensation.

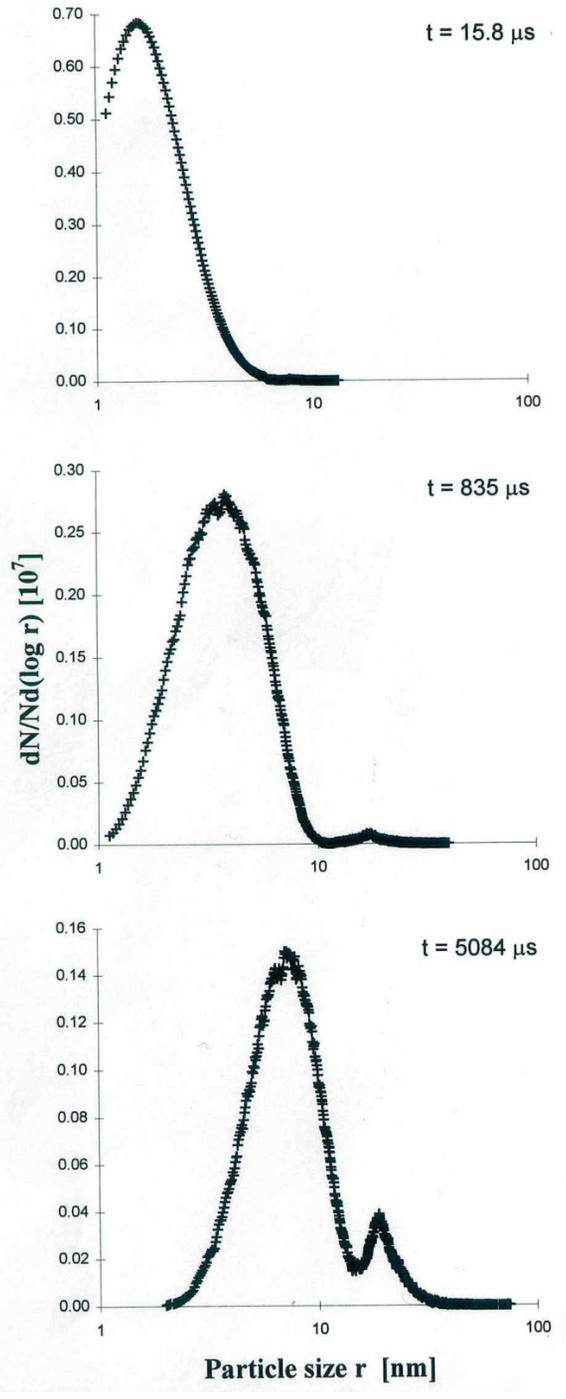

Figure 6. Evolution of an initially lognormal aerosol with S = 1.125, r_m = 1.86 nm, σ_g = 1.45, and N = 1.6 x 10^{19} ´particles/m^3 at constant temperature (1100°C).

3.1.1. Particle composition

Figure 8 shows the particle composition of the entire population after the first ms, i.e., after the bulk of the condensation has occurred (t = 5084 μs). The plot displays particle concentration

http://dx.doi.org/10.5772/62019

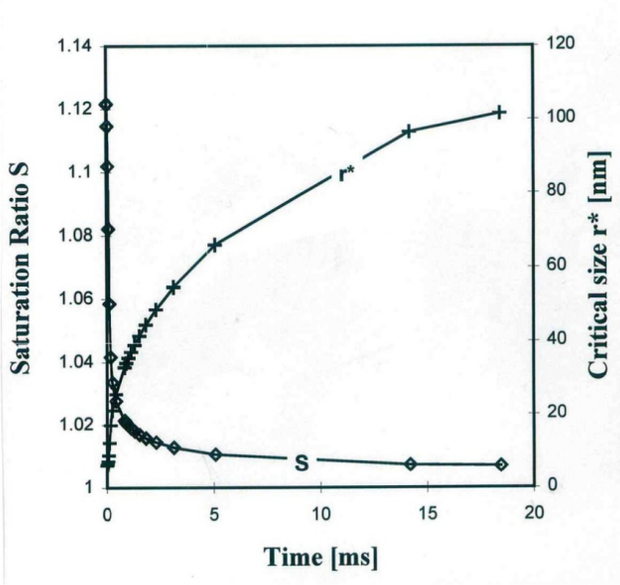

Figure 7. Evolution of S and r* for the conditions of Figure 6.

as a function of size for different compositions, and shows that composition is not a function of particle size, i.e., that for a given size there is not a unique composition. However, particles with similar composition remain grouped. For example, uncoated particles are grouped in the size range 2–12 nm. They constitute the majority of the population at this relatively early time. Thicker coatings are grouped in upper part of the distribution (r > 12 nm).

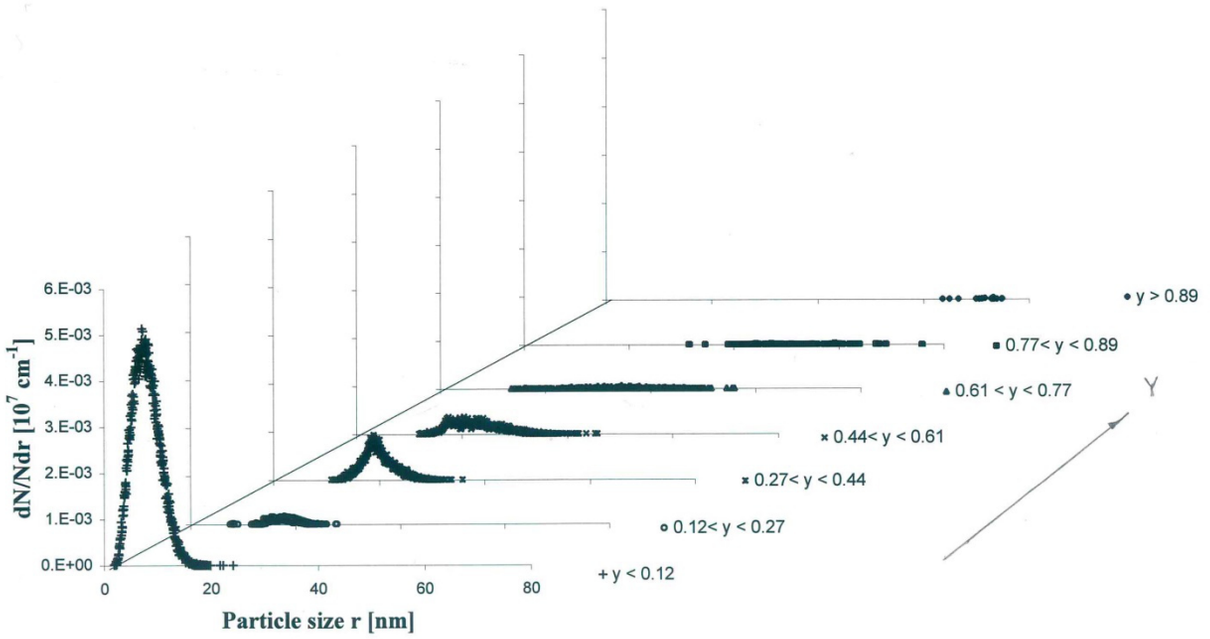

Figure 8. Particle composition for the conditions of Figure 6 at t = 5084 μs.

3.1.2. Core size distribution

The effect of the encapsulation process on the core size distribution can also be observed through the Markov-MC simulation. Figure 9 shows for the same conditions of Figure 6, the frozen and equilibrium core size distribution at 835 μs and 5084 μs, and compares them with the total particle size distribution. The frozen solution is characterized by a very high concentration of cores at $r \sim r_{mo}$ when the bulk of condensation has ceased. r_{mo} is the mean size of the particles at the onset of condensation. This is because with the frozen solution, the size of the uncoated particles is preserved when they collide with coated particles. The equilibrium core size distribution is similar to the particle size distribution when only coagulation occurs. However, the presence of the coating increases the *apparent* core size and the probability of collision of the coated particles increases. Consequently, the distribution has a higher concentration of particle for $r > r_m(t)$ compared to the lognormal distribution. Figure 9 also shows that the equilibrium core size distribution is unimodal, while the presence of the coating creates a bimodal distribution for the total particle size.

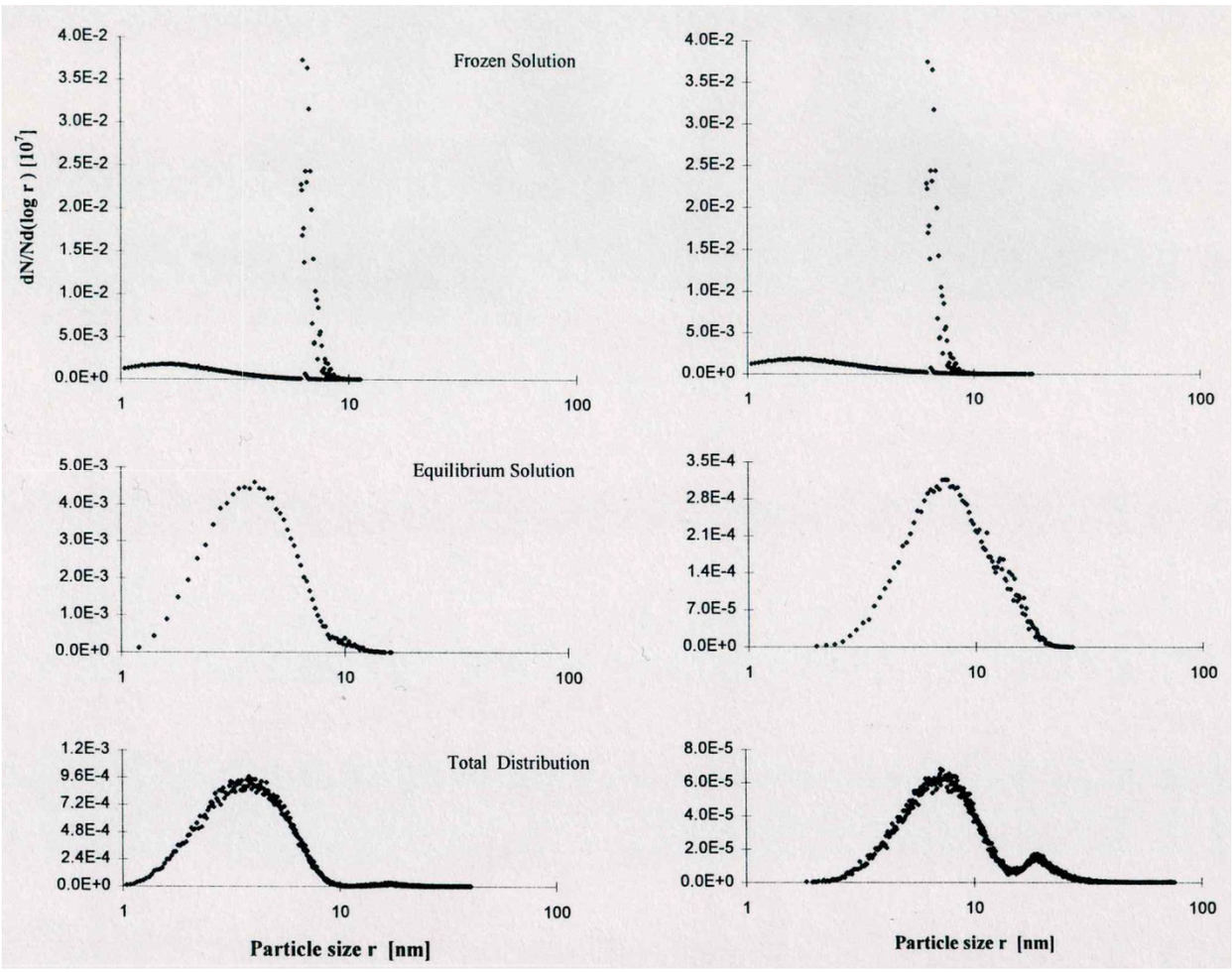

Figure 9. Frozen and equilibrium primary core size distribution for the conditions of Figure 6 at a) t = 835 μs and b) t = 5084 μs.

http://dx.doi.org/10.5772/62019

3.1.3. Evolution of a single tag particle

The Markov-MC simulation also allows the evolution of a single particle in the aerosol to be observed. Figure 10 shows the evolution of a typical particle in the aerosol (initial size r_o = 6 nm,). It shows that the particle grows by condensation (r^*_o = 5 nm) and coagulation up to r = 15.6 nm in 5 ms. The growing process involved 15 collisions. Figure 14 shows that during this time interval, the tag particle collides only with uncoated particles. It also shows that the amount of NaCl in the tag particle at the moment of collision is minor (y < 0.1).

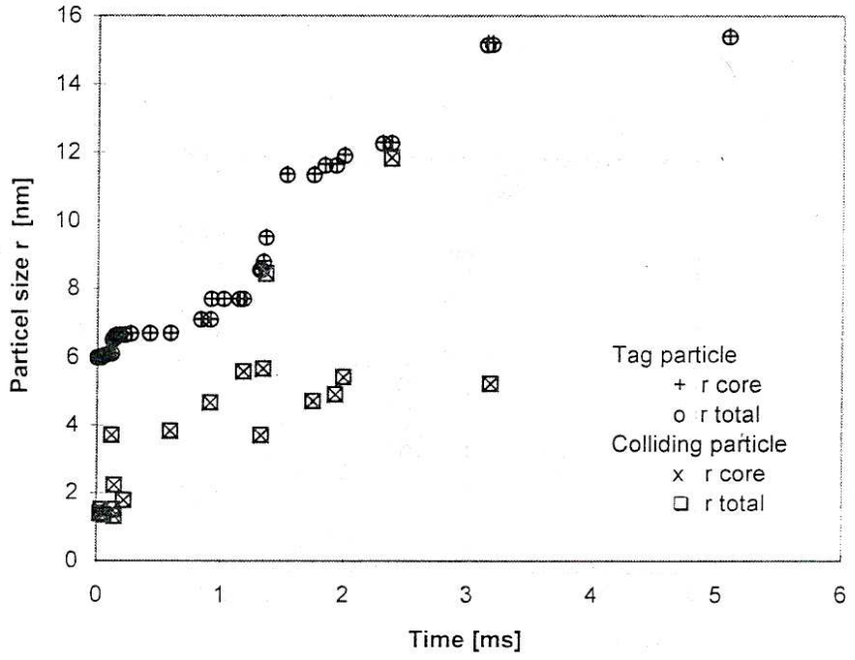

Figure 10. Evolution of a tag particle (r_o = 6 nm) during the encapsulation process for the conditions of Figure 6. "o" and "+" are the radii of the tag particle with and without NaCl encapsulation, respectively, at the moment of collision. "□" and "x" are the size of the colliding particles with and without NaCl encapsulation, respectively, at the moment of collision.

3.1.4. Discussion

The results obtained show that condensation is characterized by a very short initial high rate of condensation followed by a long period of slow condensation. For the conditions presented, the coated particles pose a light coating. The fraction of particles being coated can be estimated through the cumulative distribution function (F) by assuming that the particles prior to the onset of condensation are lognormally distributed. Figure 11 shows the fraction of particles in a lognormal distribution with size smaller than r/r_m. Thus, $1\text{-}F((r^*/r_m)_o)$ is the fraction of particles being coated. $(r^*/r_m)_o$ is the ratio of the critical particle size and mean particle size of the distribution at the onset of condensation. Therefore, for the conditions presented, only a small percentage of the population is coated directly.

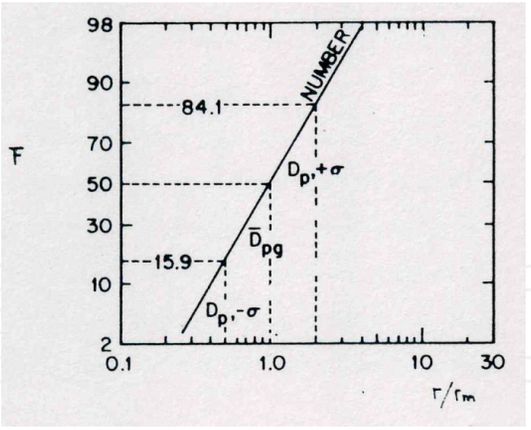

Figure 11. Number of particles in lognormal distribution with size smaller than $r_{/rm}$. 1- $F((r^*/r_m)_o)$ is the fraction of particles being coated for a given $(r^*/r_m)_o$ in an aerosol at constant temperature that experience an instantaneous change in the vapor-phase saturation conditions. $(r^*/r_m)_o$ is the ratio of the critical particle size and mean particle size of the distribution at the onset of condensation. (From Reference 64)

Allowing the aerosol to evolve further would result in collisions between coated and uncoated particles and would thus produce *encapsulated* particles. Nonetheless, it is useful to determine conditions where it is possible to directly coat a greater percentage of particles in the aerosol. Alternatively, we will consider conditions where the rate of particle growth due to coagulation is much higher than the rate of condensation, i.e., conditions for S(T) and N(t) are sought such that the rate of growth of r_m is higher than the rate of growth of r*. The rate of growth of r_m is proportional $1/\tau_{coll}$, while the rate of growth of r* is proportional to $N/\tau_{cond.}$ Table 4 shows values for τ_{cond} and τ_{coll} for a Ti/NaCl/Ar aerosol at 1100°C. From here, it can be concluded that for these conditions, the rate of condensation is much higher than the rate of coagulation, at least initially, when S is relatively large.

S	r* [nm]	N_0 [Particles/m³]	τ_{coll} [μs]	τ_{cond} [μs]
1.200	3.8	5.08×10^{18}	214	20.4
1.125	5.9	1.29×10^{18}	674	51.9
1.048	15.0	7.55×10^{16}	730	354

Table 4. $TiCl_4 + 4Na + aAr \rightarrow 4NaCl + Ti + aAr$. 1100°C

Equation 1 and Table 1, from Chapter 4, show that the rate of growth of r_m increases with N and $T^{1/2}$. However, the rate of growth of r* also increases with N and $(P\text{-}Ps)/ T^{1/2}$. Therefore, this analysis shows that for high values of S (S > 1.1), the rate of growth of r* is many orders of magnitude higher than the rate of growth of r_m. At higher temperatures, direct coating is more effective. Nonetheless, the extent of this improvement is minor. At higher temperatures, the amount of available condensable material is small and only a very light coating thickness can be obtained.

http://dx.doi.org/10.5772/62019

In principle, it might be possible to exploit the very fast rate of bulk condensation and rapidly coat most of the particles by suddenly increasing S so that $r^* << r_m$. The desire effect might be obtained by dropping the temperature of the aerosol instantaneously, (e.g., by passing the aerosol through a wave expansion) or by sweeping the aerosol in a region of high NaCl concentration. In practice, the extremely high number densities in flames ($N \sim 10^{18}$ particles/m^3) make this process impractical because the timescale for coating is microseconds. Thus, the step change in S would have to occur on a submicrosecond timescale.

3.2. Encapsulation at constant heat loss

The results for a constant temperature aerosol have demonstrated a number of observations that are essential toward understanding nano-encapsulation in flames or other aerosols with similar high number densities. The most important observation is that because of the high number density, condensation is extremely fast even if only the tail of the size distribution is coated. Since r* grows as S decreases, the largest particles receive most of the subsequent coating and smaller particles remain uncoated, until they collide with the larger coated particles. Furthermore, since for condensation to occur, S = l is the lowest value of S, in constant temperature aerosols most of the condensable material will remain indefinitely as vapor, i.e., S = l at the flame temperature gives the lowest possible vapor pressure.

In practice, the environment downstream the flame zone is not at constant temperature. Radiative and convective heat loss can result in substantial heat loss from the aerosol. Heat loss potentially is quite beneficial to nano-encapsulation as can be understood by considering the two concerns discussed above when temperature is constant. First with heat loss, r* reduces as temperature decreases. This will allow more particles to be directly coated. Second, with the resulting decrease in temperature, virtually all the condensable vapor will eventually condense out.

Initially, the aerosol is assumed to consist of a normal distribution of pure Ti particles embedded in a saturated gas-phase mixture of NaCl (S = 1.0) at 1100°C. This would be consistent with the conditions expected at the flame front for the experimental results in Chapter 2. The parameters of the distribution are assumed to be $r_m = 2.5$ nm and $\sigma = 0.4$. For these conditions, the total particle concentration is $N = 10^{18}$ particles/m^3.

For the same aerosol mass, several runs were made to study the effect of the initial distribution and the choice of this size on the evolution of the aerosol. The characteristics of the evolution of an aerosol subject to pure coagulation were discussed in Chapter 4, and therefore will be omitted here, but the key observation was that the aerosol distribution quickly evolves to a distribution that is not a function of the initial size distribution.

The time required for a coagulating aerosol to reach a given r_m can be estimated by Markov-MC simulating the evolution of an initially monodisperse aerosol. Figure 12 shows the evolution of r_m as coagulation occurs. It also shows the reduction in the particle concentration during coagulation. Figure 12 has been nondimensionalized such that it is independent of the physical properties of the aerosol; however, it is limited to aerosol in the FMR.

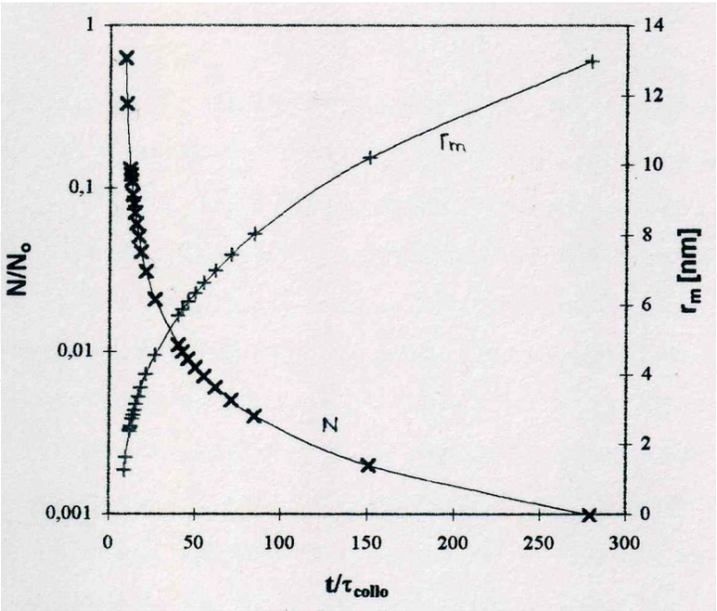

Figure 12. Time required for an initially monodisperse coagulating aerosol to reach a given r_m as simulated by the Markov-MC model.

The outputs from pure coagulation were taken as the initial conditions just prior to condensation, and the evolution of the aerosol subject to heat loss was observed. Figure 13 shows the evolution of the aerosol when the initial mean size is r_m~25 nm and the rate of heat loss is 10^{-6} W/m^3. Heat loss of 10^{-6} W/m^3 is high but reasonable for these heavily particle-laden flames. As temperature decreases, the vapor becomes supersaturated and condensation occurs over the large particles in the aerosol. Initially, the rate of bulk condensation is smaller than the rate of cooling. Therefore, as seen in Figure 14, S increases, r* decreases, and the number of particles receiving condensation increases. As the number of particles being encapsulated increases, the cooling process is retarded by the increase in the latent heat release. Soon a balance between the rate of heat loss and the bulk condensation rate is established. S approaches a maximum and r* a minimum. This minimum determines the percentage of the particles being coated. When the aerosol temperature approaches the melting point of the condensable material, the saturation pressure curve of the condensable material becomes less steep (see Figure 2) and the inverse process occurs. S becomes smaller and r* larger. The code was stopped at 100 ms as all the NaCl had condensed o_ut by this time.

The net effect on the particle size distribution and particle composition is shown in Figure 13. For the conditions and times of this simulation, condensation and coagulation are equally important (τ_{cond}~τ_{coll}). At the early stages, the interaction of coagulation and condensation creates small perturbations in the tail of the particle size distribution. The perturbations could be created due to the changes in dr*/dt relative to dr_m/dt. Coagulation decreases the concentration of small particles and magnifies these perturbations, creating a characteristic pattern. For the initial conditions chosen a 4-modal distribution is created. When r* reaches its maximum, condensation persists only on a very small fraction of particles, creating a big gap between this fraction of large particles and the main distribution. Alternatively, the perturba-

http://dx.doi.org/10.5772/62019

tions could be an artifact of the Markov-MC model. Several runs were made varying the type of grid, number of sections per unit length, and number of parcels. In all the cases, the same pattern was obtained. Further studies are required to understand the nature of these characteristic patterns.

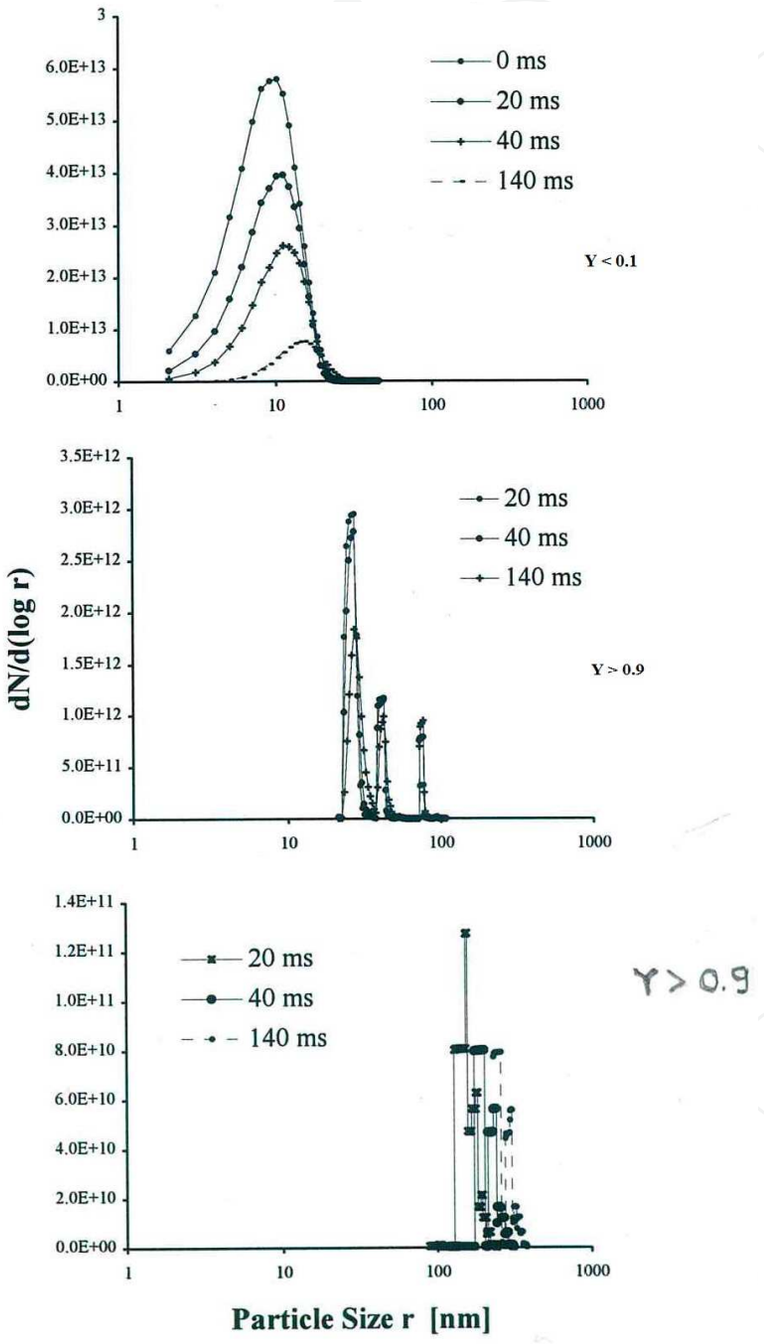

Figure 13. Evolution of particles with (a) Y < 0.1, (b) 0.1 < Y < 0.925, and (c) Y > 0.925 in a Ti/NaCl/Ar aerosol initially at 1100°C with r_m = 25 nm, S = 1.0, and N1.38 x 10^{15} particles/m^3, subject to heat loss of 10^{-6}W/m^3. The initial distribution is the one obtained after coagulation of the aerosol, starting from a normal distribution with r_m = 2.5nm, and N = 1.0 x 10^{18} particles/m^3.

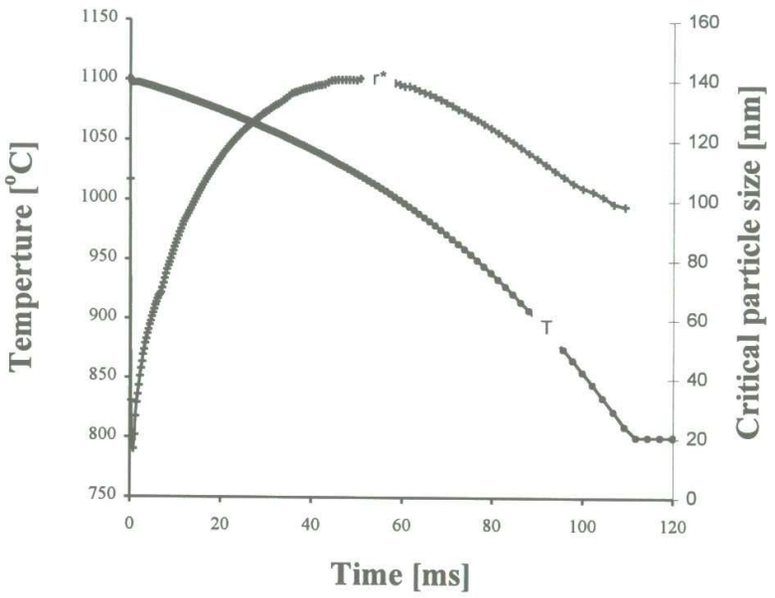

Figure 14. Evolution of r* and T during condensation at constant heat loss for the conditions of Figure 13.

The results show that by cooling the aerosol at rather high but realistic rates, only a fraction of the particles in the aerosol are initially coated and these particles contain most of the condensable material. The following discussion evaluates conditions for coating a greater fraction of particles when the aerosol is subject to constant heat loss.

Neglecting the Kelvin effect, the rate of condensation in the FMR is only a function of temperature and the physical properties of the condensable material. Therefore, for a given mass of aerosol and a given heat loss rate, the fraction of particles being encapsulated depends on particle concentration. The mean size of the core particles for a given N is determined by mass conservation.

To maximize the number of particles initially coated, values of N that make S a maximum but are below S_{crit} during the cooling process are sought. High values of N increase the rate of bulk condensation since the surface area for condensation increases. Thus, the concentration of condensable material rapidly decreases. Furthermore, the latent heat release retards the cooling process and consequently the rate of increase of S. Both processes force S to quickly approach unity, which leads to a low fraction of particles being encapsulated.

For low values of N, particle size increases but the surface area for condensation is smaller. Since the latent heat release is similar in both cases (because there is a balance between heat loss and condensation rate), the number of particles initially coated is approximately the same but the percentage of the particles being coated is greater in this case.

Several simulations were performed to establish a relationship between N and the percentage of particles initially coated and the results are shown in Table 5. These results were obtained for the same initial conditions as for Figure 13.

Rm[nm]	N[particles/m^3]	% initially coated particles
2.5	1.38E+18	0.5
5.0	1.18E+17	1.7
10	2.39E+16	6.7
25	1.53E+15	20.0
50	1.91E+14	81.0

Table 5. Relationship between N and the percentage of coated particles during 100 ms for an aerosol initially at 1100°C and S = 1.0 subject to heat loss of 10^{-6} W/m^3.

Table 5 shows for this rate of heat dissipation, most of the particles can be encapsulated when the particle concentration is low, i.e., when the particles are large. Since the percentage of coated particles for a given N is a weak function of the particle size, it is possible to have high percentage of encapsulation with particles of smaller size by controlling the concentration of the reactants such that N~10^{14} particles/m^3 for the desired value of r_m. However, this limits the production rates and requires high levels of reactant dilution for small core particle sizes.

3.2.1. Coagulation after condensation

When the aerosol temperature is significantly below T_{sat}, the condensable vapor has been depleted, condensation ceases, and coagulation after condensation is the dominant process. During this time period, indirect encapsulation of the particles occurs via coagulation of the coated particles with the uncoated particles. To study this process, the results from the previous runs were taken as initial conditions, and the evolution of the aerosol was observed. Temperature was held constant at 800°C. Figure 15 shows the evolution of the aerosol for different particle compositions. Initially, most of the particles have composition Y < 0.1. Preferential coagulation of the large, heavily coated particles (Y > 0.92) with the small uncoated particles occur ($Z \sim \beta_{ij} N_i N_j$ and β_{ij} is the greatest for the combination of large and small particles) and therefore the uncoated particles become encapsulated within the coated particles. Middle size particles begin to coagulate when the concentration of small particles has decreased (small-middle size particles first and large-middle size particles later). Coagulation fills out the gaps in the particle size distribution. Eventually, all the particles in the aerosol will collide with the large heavily coated particles. The concentration and size of the large particles remains approximately constant during the coagulation process. A very large number of small particles are required to change their size significantly. Therefore, particle size and concentration after long times can be estimated by the size and concentration of this group of large particles. Figure 15 shows that for the conditions chosen, the final NaCl particle size is r_f~300 nm and the final concentration is N_f~10^{14} particles/m^3. Experimental observation indicates that the final NaCl particle size is ~150 nm.

Considering the frozen solution, Figure 16 shows the percentage of particles being encapsulated as a function of time. It shows an exponential behavior with 90% of the particles being encapsulated within the first ~600 ms. This shows that coagulation after condensation ensures

that most of the particles are encapsulated within a time period comparable to the typical experimental residence times(>1 s).

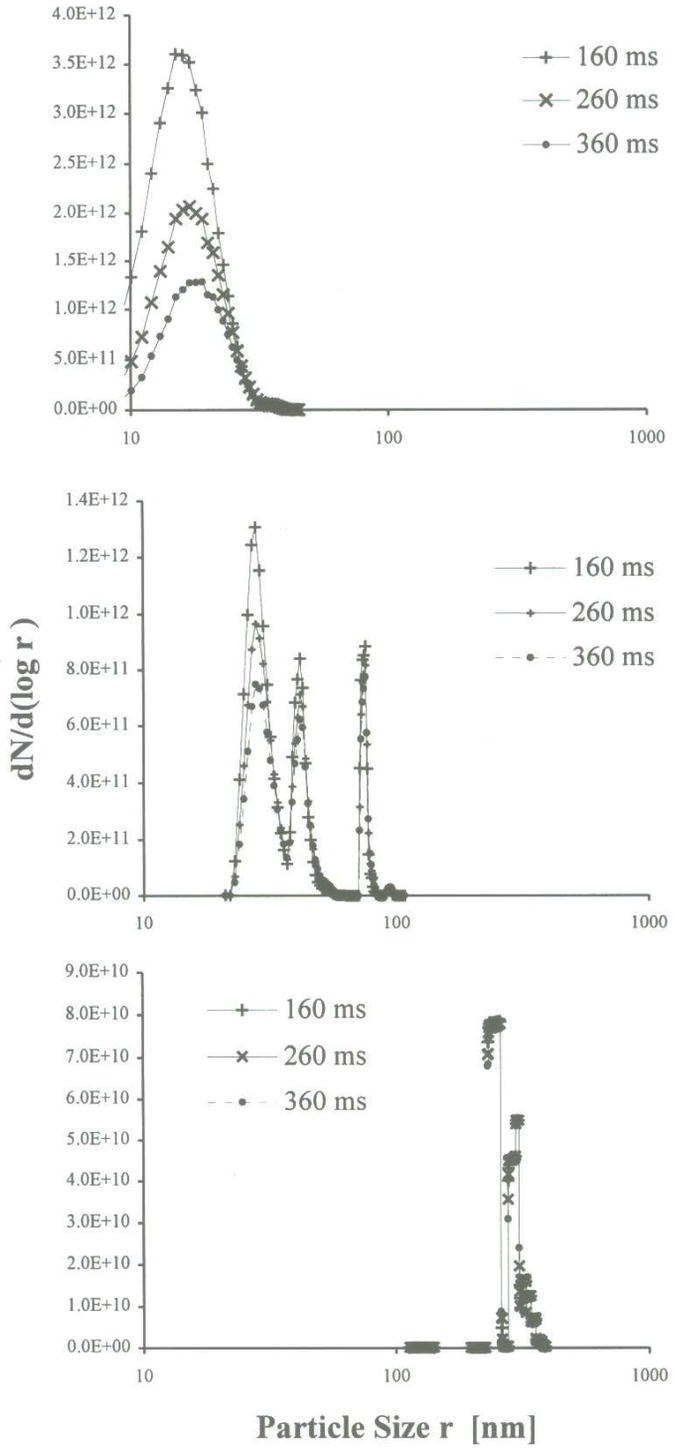

Figure 15. Evolution of the aerosol as function of particle composition with composition (a) Y < 0.1, (b) 0.1 < Y < 0.925, and (c) Y > 0.925 at t = 160, 260, and 360 ms after condensation has been completed for the conditions of Figure 13. Temperature was held constant at 800°C.

http://dx.doi.org/10.5772/62019

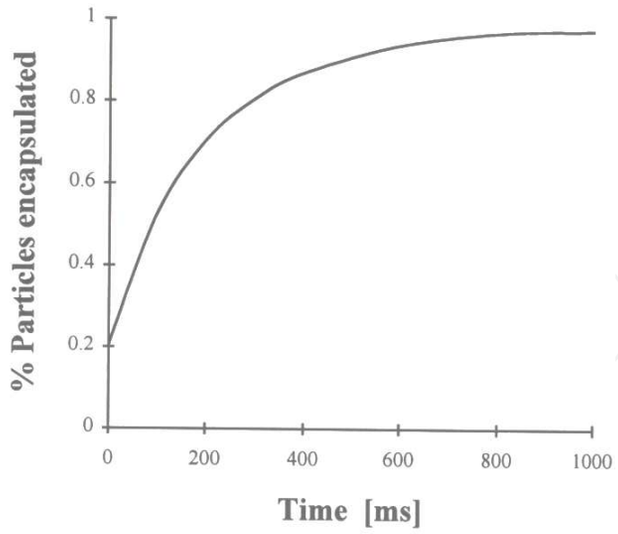

Figure 16. Percentage of particles being encapsulated via coagulation of the uncoated particles with the coated particles for the conditions of Figure 15.

3.2.2. Discussion

The results of the numerical simulation do not predict the concentration and size of the core particles. However, they can be estimated as follows: According to Table 5 and Figure 15, ~10^{14} NaCl particles/m^3 of size r~300 nm are formed by the time that most of the Ti particles have been encapsulated. Assuming that the mean size of the Ti particles at the beginning of the cooling process is r_m~25 nm, Table 5 predicts that ~20% of the 10^{15} particles/m^3 are coated at the end of the condensation process. Therefore, during the subsequent coagulation process, in average each coated particle coagulates with 5 uncoated particles, and these 6 core particles will coagulate within the NaCl matrix (see section 6.2.1). Therefore, the final size of the particle is ~$5^{1/3}$ r_m = 43 nm. Experimental results show 35 nm single core Ti particles within a NaCl droplet of ~150 nm (see Figure 9, Chapter 9). Approximately 10 AlN particles of size 24 nm within a NaCl particle[43] have been observed. This is expected since, for 24 nm there are ~10^{15} particles/m^3 and therefore for the same final number of NaCl particles there must be ~10 particles per NaCl particle.

Furthermore TiB_2 results show ~100 nm NaCl particles with hundreds of r~3–6 nm TiB_2 particles.[26] Again, this is expected since for the same final number of NaCl particles there are 100–1000 more 3–6 nm TiB_2 particles. The previous results show qualitative agreement with experimental results. This demonstrates the ability of the Markov-MC model to simulate particle dynamics in two-component aerosols.

4. Summary

A phenomenological description of the particle encapsulation method observed in sodium/halide flames has been presented and the Markov-MC model has been used to study the

evolution of an M/NaCl/Ar combustion aerosol. Nano-encapsulation is obtained directly by condensing the second phase material (NaCl) over the M core particles, producing coated particles, and indirectly via coagulation of the uncoated particles with coated particles. Direct encapsulation occurs through heterogeneous condensation of supersaturated vapors.

Particle encapsulation at constant temperature was studied. The results are characterized by a very short initial high rate of condensation followed by a long period of slow rate of condensation. Only a very small percentage of the population is coated, and the encapsulated particles possess a very light coating. The alternatives to increase the number of particles being encapsulated and the thickness of the encapsulation are not practical or feasible. Encapsulation when the aerosol is subject to constant heat loss was studied. This process exploits the facts that by dropping aerosol temperature more condensable material is available for encapsulation and more particles are directly encapsulated since r* obtain lower values. Results show that only a small fraction of the particles receive most of the condensable material. The concentration and size of these particles determine the final size and concentration of the NaCl particles. Conditions to encapsulate most of the particles during the cooling process were sought. It was found that for the same mass of aerosol, the percentage of coated particles can be increased by decreasing particle concentration. Encapsulation of uncoated particles via coagulation with the coated particles was also studied. Results show that 90% of the particles can be encapsulated within a time period comparable to the typical experimental residence time. Numerical results for particle size and number of particles within a NaCl particle show good agreement with experimental observations for Ti, AIN, and TiB_2. This work has gained substantial understanding in the particle encapsulation process and has shown the usefulness of the Markov-MC model to study two-component aerosols.

Author details

Jose Ignacio Huertas

Address all correspondence to: jhuertas@itesm.mx

Tecnológico de Monterrey, Mexico